Journal of Proteomics 270 (2023) 104739

Contents lists available at ScienceDirect

Journal of Proteomics

journal homepage: www.elsevier.com/locate/jprot

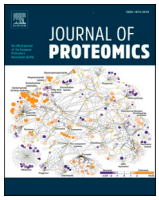

Proteomic changes associated with maternal dietary low ω6:ω3 ratio in piglets supplemented with seaweed Part II: Ileum proteomes

Thi Xuan Nguyen [a,b,d,*], Alessandro Agazzi [a], Suzanne McGill [b], Stefan Weidt [b], Quang Hanh Han [b,d], Andrea Gelemanović [c], Mark McLaughlin [b], Giovanni Savoini [a], Peter David Eckersall [b], Richard Burchmore [b]

[a] Università degli Studi di Milano, Via dell'Università, 6, 26900 Lodi, Italy
[b] University of Glasgow, Bearsden Rd, G61 1QH, United Kingdom
[c] Mediterranean Institute for Life Sciences (MedILS), Meštrovićevo šetalište 45, 21000 Split, Croatia
[d] Vietnam National University of Agriculture, Hanoi, Viet Nam

ARTICLE INFO

Keywords:
Ileal proteome
ω6:ω3 fatty acids
Seaweed
DNA and protein synthesis
Weaned pigs
Epithelial cells

ABSTRACT

This study evaluates how long-term dietary low ω6:ω3 ratio in sows and offspring's seaweed (SW) intake affects piglet intestinal function and growth through modifying ileum proteome. Sows were assigned to either control diet (CR, ω6:ω3 ratio = 13:1) or treatment diet (LR, ω6:ω3 = 4:1) during gestation and lactation ($n = 8$ each). The male weaned offspring were received a basal diet with or without SW powder supplementation (4 g/kg) for 21 days, denoted as SW and CT groups, respectively. In total, four groups of weaned piglets were formed following maternal and offspring's diets combination, represented by CRCT, CRSW, LRCT, and LRSW ($n = 10$ each). Piglet ileum tissue was collected on day 22 post-weaning and analysed using TMT-based quantitative proteomics. The differentially abundant proteins ($n = 300$) showed the influence of maternal LR diet on protein synthesis, cell proliferation, and cell cycle regulation. In contrast, the SW diet lowered the inflammation severity and promoted ileal tissue development in CRSW piglets but reduced the fat absorption capacity in LRSW piglets. These results uncovered the mechanism behind the anti-inflammation and intestinal-boosting effects of maternal LR diet in piglets supplemented with SW.

Significance

Weaning piglets undergo significant developmental changes in intestinal maturation. This is the first study on the ileum proteomic changes associated with maternal dietary low ω6:ω3 ratio in piglets supplemented with seaweed. Present research assists in understanding the molecular mechanism regarding previously reported performance and oxidative status data in piglets (already published elsewhere). The results highlight the importance of nutritional management from the early stage (sows and newborn progeny) until later (post-weaning) to maintain piglet intestinal health and productivity.

1. Introduction

In pigs, weaning is a stressful event linked to significant intestinal changes [1]. Weaning stress triggers pro-inflammatory responses and stimulates epithelial proliferation (renewal) and differentiation, resulting in increased crypt depth, reduced intestinal villous height, and higher proportion of immature epithelial cells [1]. This process is essential to ensure an effective barrier function of the small intestine [2] and to progressively educate the mucosal immune system upon the antigenic challenge for health and normal growth maintenance [3]. Piglets in this critical phase must be well-equipped to protect the intestines and immune development, preventing an excessive reduction in feed consumption, intestinal inflammation, and dysbiosis [4].

Maternal effects include the environment experienced by the mother and nutrients belonging to the early life period that considerably influences offspring phenotype and growth [5,6]. Unbalanced maternal nutrition would lead to a mismatch in the maternal-offspring environment, suboptimal offspring growth [7], and health problems associated with metabolic dysfunction [8]. In pigs and mammals, the maternal effects continue during the lactation period and only stop when the

* Corresponding author at: Università degli Studi di Milano, Via dell'Università, 6, 26900 Lodi, Italy.
E-mail address: thixuan.nguyen@unimi.it (T.X. Nguyen).

https://doi.org/10.1016/j.jprot.2022.104739
Received 25 March 2022; Received in revised form 14 September 2022; Accepted 16 September 2022
Available online 27 September 2022

piglets are weaned. Therefore, the role of maternal nutrition is vital for offspring in response to early life stimuli [9], such as weaning stress. There have been no studies exploring the underlying mechanism of maternal-offspring nutritional interventions in initiating the development of piglets' ileal epithelial cells.

A modern human diet containing a high ω6:ω3 fatty acid ratio (~20:1) is associated with elevated pro-inflammatory mediators from ω6 and decreased the anti-inflammatory mediators from ω3, leading to excessive inflammation [10,11]. Consequently, lowering the dietary ω6:ω3 ratio might be a promising approach to decrease inflammation and allergies [12] and maintain good health [13]. Maternal dietary low ω6:ω3 ratio in swine with more ω3 fatty acids supplemented from linseed oil is effective in enhancing weaning survival rate [14], postnatal growth, and metabolic traits [14–16]. Besides, the post-weaning diet program is a crucial determinant of lifelong health and performance [17]. The brown seaweed *Ascophyllum nodosum* is a potential prebiotic and antibacterial dietary supplement for swine thanks to its high content of bioactive compounds such as fucoidan (a type of polysaccharide) and laminarin [18]. Dried *A. nodosum* supplementation at 2.5, 5, and 10 g/kg for weaned piglets did not affect performances, plasma oxidative status, gut morphology, and health [19]. Supplementing piglet diets with 5, 10, and 20 g/kg *A. nodosum* extract improved growth but had no positive effect on immune responses to *S. typhimurium* challenge [20]. However, weaned piglets supplemented with 10 and 20 g/kg of dried intact *A. nodosum* had improved performance and gut health through a beneficial shift in the microbial population [21]. Nevertheless, the combined effects of maternal low ω6:ω3 ratio and offspring *Ascophyllum nodosum* diets on the molecular mechanism underlying offspring development are complicated and not addressed in swine.

Here, to better understand the mechanism behind effects of early- (maternal low ω6:ω3 intake) and later-life nutritional programming (offspring seaweed supplementation) on post-weaned piglet's ileal development, a Tandem Mass Tag (TMT)-based quantitative proteomics approach was applied. It was hypothesized that maternal-offspring dietary treatments would accelerate the ileal development in weaned piglets and relieve weaning distress through modifying the ileal protein profile. This study brings new insights into ileal developmental changes during post-weaning periods, which were affected by the associations between long-term maternal and offspring dietary treatments. The data in the current research (Part 2) provides additional evidence on piglets' dynamic molecular response to interactions between maternal low ω6:ω3 intake and post-weaned seaweed supplementation (Part I was on serum proteome, submitted).

2. Materials and methods

2.1. Animals and sample collection

A feeding trial was performed with 40 male weaned piglets at the Animal Production Research and Teaching Centre of the Department of Veterinary Medicine and Animal Science, University of Milan (Lodi, Italy). The experiment protocol was approved by the Ethical Committee of the University of Milan (OPBA 67/2018) and the Italian Ministry of Health (authorization n. 168/2019 PR). The study design and zootechnical data were previously reported by Nguyen et al. [14].

After separating from the mothers, piglets weighing 6.46 kg (± 0.15) (mean ± SE) at day 26 (± 1.76) of age were selected from different mothers within a group, among two groups receiving either a control ratio of ω6:ω3 fatty acids (CR, 13:1 during gestation and 10:1 during lactation) or a low ratio (LR, 4:1, during gestation and lactation). Piglets were provided a basal commercial diet [14] and supplemented with or without 4 g seaweed powder *(A. nodosum;* Prodotti Arca S.r.l, Monza, Italy) per kg of feed, namely SW and CT groups, respectively. In total, four groups ($n = 10$ each) were formed: CRCT, CRSW, LRCT, and LRSW. At the end of the post-weaning (PW) period (day 22), piglets were sacrificed to harvest whole ileum samples (~3 cm) using 2-mL cryogenic vials (Nalgene™, Thermo Scientific™). The mucosa, submucosa, and muscular layer were not separated. Samples were then frozen immediately and stored at −80 °C until analysed.

2.2. Protein identification and quantification using the TMT approach

2.2.1. Protein extraction and quantification

The protein in ileum samples ($n = 5$ per group x 4 groups) was extracted according to previously published methods [22,23]. In brief, cold cut frozen ileum tissue was homogenized using mortar and pestle in liquid nitrogen. Afterward, ~200 mg of fine ileum powder was sonicated in 500 μL lysis buffer (100 mM TEAB, 2% SDS), using a probe sonicator (OPTIMA, XL 100 K, Germany) at 40% amplitude, following a sequence of 10-s on and 5-s off, three times on ice. The obtained homogenate was centrifuged at 14,000 ×*g* for 30 min at 4 °C. The supernatants (ileum extract) were separated from the pellets and total protein concentration was determined by the bicinchoninic acid method (BCA Assay, Pierce™ BCA Protein Assay Kit, Thermo Scientific, Meridian Rd., Rockford, IL, USA) with bovine serum albumin as standard. Samples were prepared and kept at −80 °C before analyses.

2.2.2. Protein digestion and TMT labelling

Tandem Mass Tag (TMT) labelling quantitative approach was applied to analyse the proteomic profiling of ileum samples as described previously [24]. 100 μg of protein (~4.63 μL) per sample was processed using the "in-solution" filter-aided sample preparation (FASP) with 10 kDa molecular weight cut-off filters (Merck Millipore, Carrigtohill, Ireland). Protein was denatured with 4% SDS and reduced using 0.1 M Tris/HCL pH 7.6 and 0.1 M dithiothreitol (DTT) (Sigma Aldrich, St. Louis, MO, USA). Alkylation of cysteine residues was performed using 0.05 M Iodoacetamide (IAA) (Sigma Aldrich, St. Louis, MO, USA) in the dark for 20 min at room temperature. Tryptic digestion was performed at 37 °C overnight using 1 μg of trypsin (Promega, Madison, WI, USA, 1:37) and then stopped using 1% trifluoroacetic acid (TFA) before vacuum-dried at 45 °C. The obtained peptides were labelled with freshly prepared TMT11plex (Thermo Fisher Scientific, Rockford, IL, USA), incubated for 60 min, quenched in 45 min and vacuum centrifuged until completely dry following the manufacturer's protocol. A pooled sample was prepared by taking an equal amount of peptide from each sample, labelled by a TMT tag and used as an internal standard between two TMT experiments.

2.2.3. Liquid chromatography tandem mass spectrometer (LC-MS/MS)

The labelled peptides were loaded onto a nanoflow uHPLC system (Thermo Fisher Scientific RSLCnano, Horsham, UK), detected using electrospray ionization (ESI) mass spectrometry MS/MS with an Orbitrap Elite MS (Thermo Fisher Scientific, Horsham, UK). HPLC solvents contain 20 μL of 5% acetonitrile (ACN) and 0.5% formic acid. Ionization in LC-MS interfaces using a NanoMate Triversa (Advion Bioscience, Harlow, UK) with an electrospray voltage of 1.7 kV. The peptides (5 μL) were desalted using 1% ACN and 0.1% formic acid on the trap column (0.3 × 5 mm) at a flow rate of 25 μL/min for 12 min.

The purified peptides were then enriched on a Pepmap C18 reversed-phase column (50 cm × 75 μm, 3 μm, 100 Å, Thermo Fisher Scientific, Horsham, UK), and separated on an analytical column at a fixed flow rate of 0.3 μL/min. The solvent system used 0.1% aqueous formic acid as solvent A and 0.08% formic acid in 80% ACN as solvent B. Fractionation was run with 4% solvent B for 10 min, followed by 4–60% solvent B for 170 min, 60–99% solvent B for 15 min, and held at 99% solvent B for 5 min. The column was then adjusted to the initial set-up for re-equilibration (10 min) before injecting the following sample.

Eluting peptides were subjected to MS/MS analysis on an Orbitrap Elite MS. Each MS scan was within the *m/z* range of 380–1800. The top three precursor ions were fragmented using CID and HCD collision cells, detected in the Orbitrap at a resolution of 30,000 FWHM, as defined at m/z 400. Precursor ions chosen were excluded after every 180 s, and

single-charged ions were omitted from selection.

2.3. MS/MS data processing

The MS/MS data were searched against the UniProt *Sus scrofa* database (104,940 sequences; downloaded on 18/02/2021) for protein identification and relative quantification using Sequest HT search engine in Proteome Discoverer (v2.4, Thermo Fisher Scientific). The search parameters were as follows: tryptic peptides with two missed-cleavage allowed, carbamidomethylation at cysteine residue was stated as fixed modification, oxidation at methionine, deamidation at asparagine and glutamine residues, and TMT labelling at lysine residue and peptide N-terminus were stated as variable. The mass tolerance for the precursor ions was 10 ppm and that for fragment ions was 0.02 Da. A false discovery rate (FDR) of 1% was applied at the peptide level. Proteins were identified containing at least two peptides with 5% FDR. The mass spectrometry proteomics data have been deposited to the ProteomeXchange Consortium via PRIDE [25] partner repository with the dataset identifier PXD032326.

2.4. Validation of proteomics results

To validate ileum proteomics results, evaluating changes in the non-depleted sample contents of villin-1 (VIL1) and Proliferating cell nuclear antigen (PCNA) were implemented, which were chosen based on their significant abundance changes, biological meaning and antibody availability. The concentration of VIL1 and PCNA in ileum extraction samples was quantified using Western blot, detailed as described elsewhere [26]. Briefly, an amount of 2 μg and 10 μg ileum proteins per sample was used for VIL1 and PCNA immunoassays, respectively. The presence of VIL1 in ileum samples was captured and detected using rabbit polyclonal antibody to villin diluted in 1:1000 (ab233155, Abcam Ltd. UK), followed by secondary antibody conjugated donkey anti-rabbit IgG to horseradish peroxidase (HRP) diluted in 1:10,000 (ab7125, Abcam Ltd. UK). Ileum PCNA was detected using goat polyclonal antibody raised against synthetic peptide of PCNA at 1:1000 dilution (pab27564, Abnova, Taipei, Taiwan) as the primary antibody and HRP-conjugated donkey anti-goat IgG 1:5000 as the secondary antibody.

The experimental design, pipeline for proteomics analysis (containing sample preparation, TMT labelling, and LC-MS/MS, data analysis, and quantitation), and validation of proteomics are illustrated in Fig. 1.

2.5. Statistical and bioinformatics analysis

2.5.1. Statistical analysis for proteomics data

The peptide spectrum match (PSM)-level data were analysed using linear mixed-effects models with Empirical Bayes moderation on MSstatsTMT package v2.0.0 [27] in R v4.1.0 [28]. Protein was quantified based on unique peptides only and summarization using the median polish method. Protein normalization was performed using the internal standard channel. Only master proteins were subjected to the statistical analysis. Proteins were significantly changed at an adjusted p-value < 0.05 and suggestively altered at a p-value < 0.05. The Benjamini-Hochberg correction was applied to adjust the p-values ($p < 0.05$).

The volcano plots were illustrated using packages *ggplot2* v3.3.3 [29] and *ggrepel* v0.9.1, PCA plots used *ggplot2* v3.3.3 [29], PLS-DA plots used mixOmics v6.16.3 [30], and heatmaps used *pheatmap* v1.0.12. Venn diagrams were performed using web tool Venny 2.1 (https://bioinfogp.cnb.csic.es/tools/venny/) [31].

2.5.2. Bioinformatics analysis

For identified master protein, the UniProt retrieve/ID mapping tool was used to convert their accession numbers into the corresponding gene ID. For undefined proteins, their best match on *Sus scrofa* orthologue annotated genes (minimum 70% identity) were used instead using the SmartBLAST tool (https://blast.ncbi.nlm.nih.gov/smartblast/).

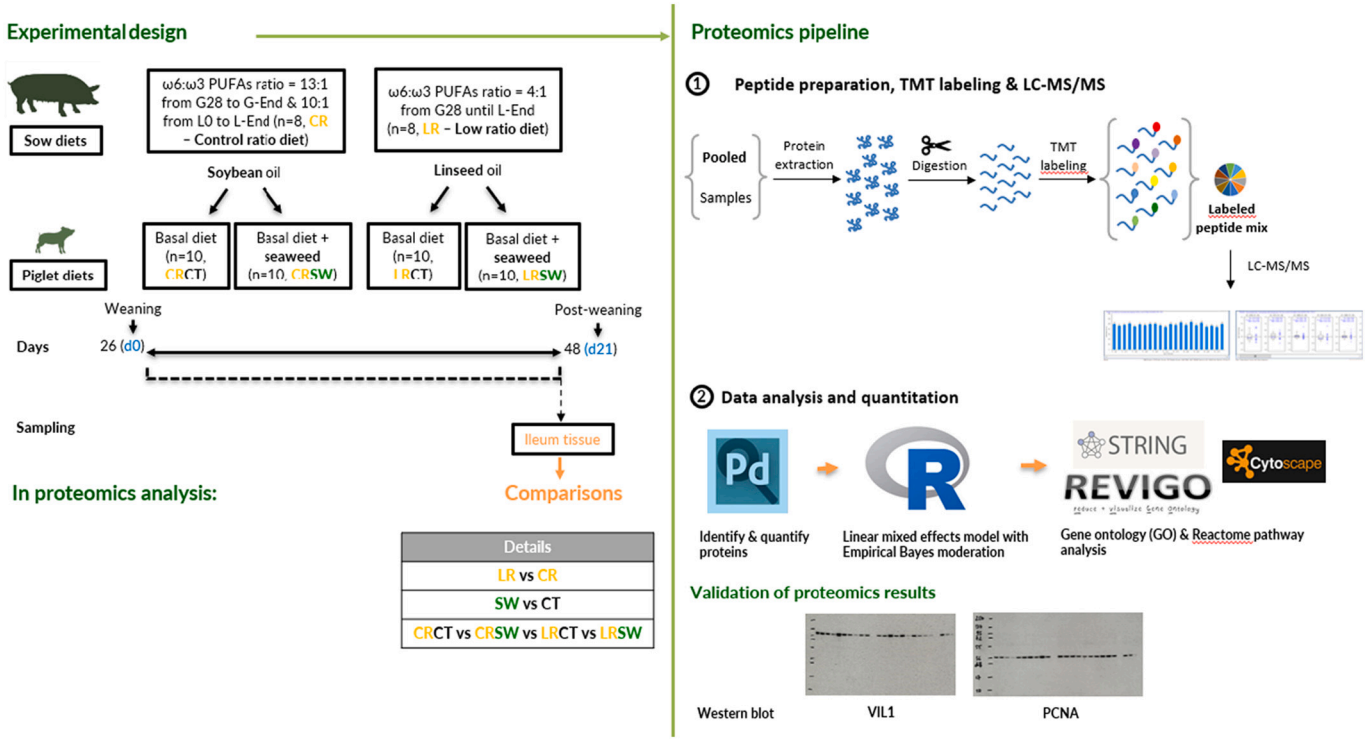

Fig. 1. The experimental design, proteomics pipeline and validation of proteomics results. Proteomics pipeline contains: (1) Peptide preparation, TMT labelling, and LC-MS/MS analysis, (2) Data analysis and quantitation: protein identification and quantitation using Proteome Discoverer, statistical analysis based on the linear mixed-effects model with empirical Bayes moderation (R package MSstatsTMT), bioinformatics analysis (Gene Ontology (GO) and Reactome pathway enrichment analysis).

Differential abundant proteins (DAPs) were imported into the STRING database v11.5 [32] and retrieved the protein-protein interaction (PPI) network, Reactome pathways, Gene Ontology (GO) analysis containing Biological Process (BP), Molecular Function (MF), and Cellular Component (CC). Extremely similar GO terms were filtered using the REVIGO [33] (revigo.irb.hr), with the following settings: whole UniProt as the database, SimRel as semantic similarity measure at a threshold of 0.5. The network showing interactions between desired Reactome pathways and DAPs between comparisons were illustrated using Cytoscape software v3.8.2 [34].

2.5.3. Statistical analysis for validation data

The validation data on VIL1 and PCNA were analysed and checked for their correlation with proteomics data. Data normalization and variance homogeneity were checked by the Shapiro-Wilk and Levene's test. Difference between groups was discovered using the linear mixed model, and *p*-values were adjusted using the Benjamini-Hochberg post hoc pairwise testing. Fixed effects were sow diet, piglet diet, time, and their interactions. The random effect was an individual piglet. Spearman correlation analysis assessed the relationship between proteomics and validation results for both VIL1 and PCNA.

3. Results

3.1. Proteomic analysis

The proteomics analysis generated 4428 features and mapped 2216 unique peptides, which represented 1237 proteins and 671 master proteins. After filtering proteins with no unique peptide, only one peptide, and singly charged ions, 300 master proteins were quantified and reserved for statistical analysis (Supplementary material_List of 300 master proteins).

3.1.1. DAPs in LR vs CR and SW vs CT groups

The DAPs were determined via two comparisons: LR vs CR and SW vs CT (Table 1). Comparison between LR and CR discovered 5 DAPs (4 increased and one decreased) and comparison SW vs CT revealed 19 DAPs (5 increased and 14 decreased) (Table 1, $p < 0.05$). No DAPs were shared between these two comparisons (Venn diagram, Fig. 2A). The DAPs were determined distinctly for comparison LR vs CR comprising increased-abundant proteins such as Glutamine–fructose-6-phosphate transaminase (GFPT1), T-complex protein 1 subunit beta (CCT2), and 40S ribosomal protein SA (RPSA), and one decreased-abundant protein (calmodulin 1, CALM1). In comparison SW vs CT, the leading increased-abundant protein was proliferating cell nuclear antigen (PCNA) and the leading decreased-abundant proteins were villin-1 (VIL1) and keratin proteins (KRT8, KRT19, KRT20) ($p < 0.05$, Table 1).

3.1.2. DAPs in the comparisons among all 4 groups (CRCT, LRCT, CRSW, and LRSW)

The PLS-DA score plot shows a mixed grouping of ileum samples from 4 groups of piglets at day 22 post-weaning (Fig. 3), containing CRCT, LRCT, CRSW, and LRSW groups. The first two variates contributed a cumulative variance rate of 33% of the overall variance. The DAPs in piglet ileum among these 4 groups are examined in six comparisons and presented in Table 2.

The unique and shared DAPs in comparing LRCT, CRSW, and LRSW with CRCT groups are indicated in the Venn diagram (Fig. 2B) and heatmap (Fig. 4). As shown in these two figures, these three comparisons shared 4 similar DAPs (3 increased and one decreased). Groups SW (CRSW and LRSW) versus CRCT group revealed 6 DAPs (3 increased and 3 decreased). Groups LR (LRCT and LRSW) versus the CRCT group yielded only one decreased-abundant protein, calmodulin 1 - CALM1.

Furthermore, the LRSW group was compared to three remaining groups (CRCT, CRSW, and LRCT) using a Venn diagram (Fig. 2C) and heatmap (Fig. 4). These two figures display only one overlap DAP

Table 1
The differentially abundant proteins (DAPs) in piglet ileum at day 22 of post-weaning of two comparisons: LR vs CR and SW vs CT.

Protein name	Gene names	Accession number[1]	Number of peptides	log2FC[2]	*P*-value
LR vs CR					
Glutamine-fructose-6-phosphate transaminase (isomerizing)	GFPT1	E1U318	2	0.32	0.042
T-complex protein 1 subunit beta	CCT2	A0A5G2QMG1	2	0.17	0.009
PDZ and LIM domain protein 7	PDLIM7	A0A4X1SEG0	3	0.16	0.026
40S ribosomal protein SA	RPSA	A0A480SME4	4	0.14	0.044
Calmodulin 1	CALM1	A0A4X1ST02	3	−0.10	0.030
SW vs CT					
Proliferating cell nuclear antigen	PCNA	X5FB24	2	0.51	0.005
Cathepsin D	CTSD	A0A480M5F4	2	0.29	0.034
Decorin	DCN	F1SQ10	4	0.19	0.009
Collagen-binding protein	SERPINH1	A0A480U2E1	10	0.09	0.002
Fructose-bisphosphate aldolase	ALDOA	A0A4X1U0N5	11	0.06	0.046
ATP synthase subunit alpha	ATP5A1	A0A287AGU2	13	−0.09	0.023
ATP synthase subunit beta	ATP5B	A0A481D142	17	−0.10	0.019
Aconitate hydratase, mitochondrial (Aconitase)	ACO2	F1SRC5	2	−0.13	0.036
Creatine kinase	CKB	A0A4X1TV43	8	−0.13	0.025
Proteasome activator complex subunit 1	PSME1	Q64L94	4	−0.18	0.018
4-trimethylaminobutyraldehyde dehydrogenase	ALDH9A1	F1S232	2	−0.23	0.025
Sodium/potassium-transporting ATPase subunit alpha	ATP1A1	A0A4X1SW39	2	−0.33	0.049
Creatine kinase U-type, mitochondrial	CKMT1B	Q29577	2	−0.40	0.048
Histone H2A	H2AFX	A0A5G2QMX0	3	−0.41	0.037
Keratin, type I cytoskeletal 19	KRT19	A0A480IFL7	11	−0.47	0.003
Keratin, type II cytoskeletal 8	KRT8	A0A4X1WBI1	18	−0.51	0.006
Enoyl coenzyme A hydratase 1	ECH1	A0A4X1T0M5	2	−0.53	0.009
Keratin, type I cytoskeletal 20	KRT20	A0A5G2QPZ4	6	−0.75	0.006
Villin-1	VIL1	Q29261	2	−0.98	0.018

[1] Accession number from UniProt protein database for *Sus scrofa*.

[2] log2FC is base 2 logarithm transformed of fold change value which represents the ratio of expression levels in the first-mentioned group vs second-mentioned group. CR: mother diet with ω6:ω3 ratio = 13:1 during gestation, starting from day 28 (G28) and 10:1 during lactation; LR: mother diet with ω6:ω3 ratio = 4:1 from G28 until the end of lactation. SW: piglet diet with seaweed supplementation, CT: piglet diet without seaweed supplementation.

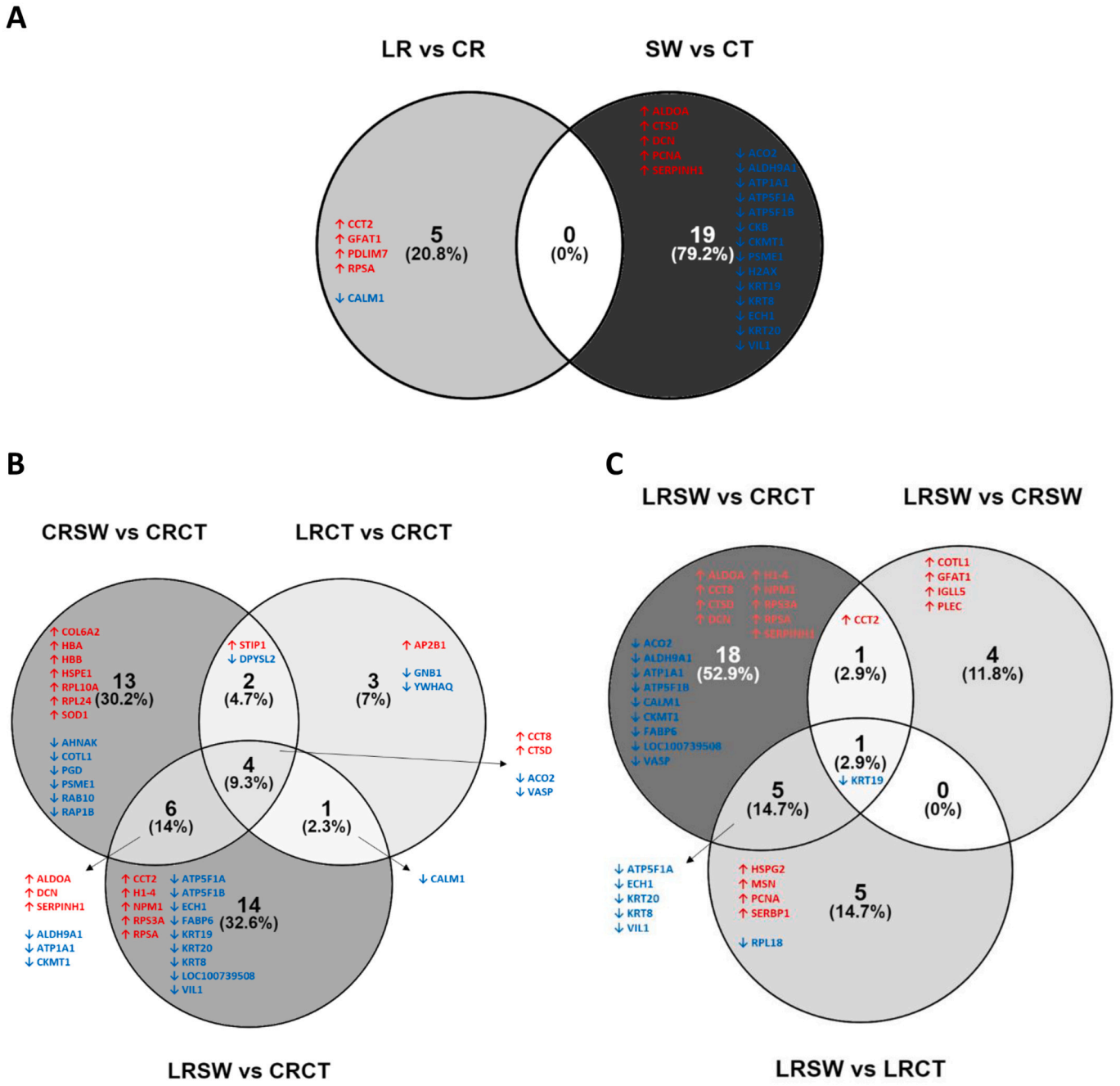

Fig. 2. Venn diagram representing separated and overlapped differentially abundant proteins (DAPs) between two comparisons of piglet ileum: LR vs CR and SW vs CT. CR: piglet born from sow fed diet with ω6:ω3 ratio = 13:1 during gestation, starting from day 28 (G28) and 10:1 during lactation; LR: piglet born from sow fed diet with ω6:ω3 ratio = 4:1 from G28 until the end of lactation. SW: piglet diet with seaweed supplementation, CT: piglet diet without seaweed supplementation. CRCT: piglets fed no seaweed (SW, *Ascophyllum nodosum*), which nursed by sows fed dietary ω6:ω3 ratio = 13:1 during gestation, starting from day 28 (G28) and 10:1 during lactation. CRSW: piglets fed SW, which nursed by sows fed dietary ω6:ω3 ratio = 13:1 during gestation and 10:1 during lactation. LRCT: piglets fed no SW, which nursed by sows fed dietary ω6:ω3 ratio = 4:1 from G28 until the end of lactation. LRSW: piglets fed SW, which nursed by sows fed dietary ω6:ω3 ratio = 4:1 from G28 until the end of lactation.

(keratin19 - KRT19), which was decreased among the three comparisons. The comparisons between the LRSW group versus CT groups (CRCT and LRCT) discovered 5 DAPs that were all decreased in abundances, such as ATP synthase subunit alpha (ATP5F1A), keratin proteins (KRT8, KRT20), and villin-1 (VIL1). Comparing the LRSW group versus CR groups (CRCT and CRSW) revealed only one DAP (T-complex protein 1 subunit beta - CCT2), which was increased in abundance. The heatmap of the DAPs of 20 samples in four groups of piglet ileum was also presented in Supplementary Fig. S10.

3.1.3. GO enrichment of all identified ileum proteins

The protein-protein interaction (PPI) enrichment analysis shows an association among 300 master proteins, with 288 nodes and 5696 edges ($p < 1.0e-16$) (Supplementary Fig. S3). The functional enrichments emphasised 172, 54, and 60 GO terms on biological processes (BP), molecular function (MF), and cellular components (CC), respectively (Supplementary Table S1). The top three enriched GO-BP terms were symbiotic process [GO:0044403], cellular localization [GO:0051641], and translational initiation [GO:0006413]. The DAPs primarily

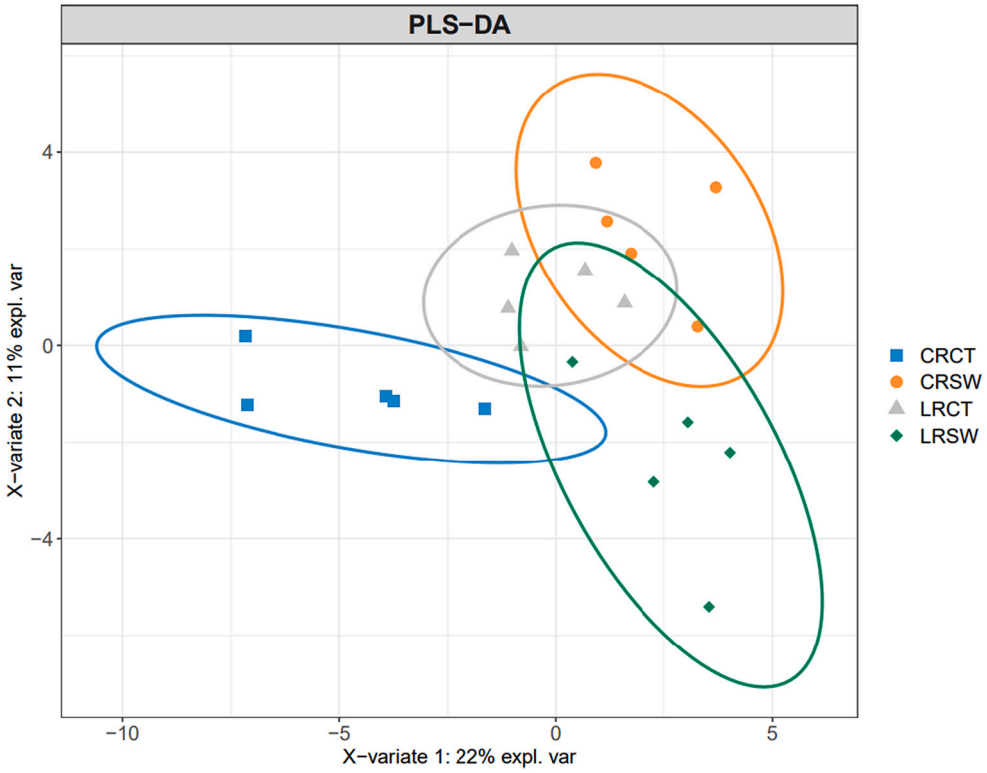

Fig. 3. Partial Least Squares Discriminant Analysis (PLS-DA) score plots showing the clustering of samples from four groups of piglet ileum containing CRCT: piglets fed no seaweed (SW, *Ascophyllum nodosum*), which nursed by sows fed dietary ω6:ω3 ratio = 13:1 during gestation, starting from day 28 (G28) and 10:1 during lactation. CRSW: piglets fed SW, which nursed by sows fed dietary ω6:ω3 ratio = 13:1 during gestation and 10:1 during lactation. LRCT: piglets fed no SW, which nursed by sows fed dietary ω6:ω3 ratio = 4:1 from G28 until the end of lactation. LRSW: piglets fed SW, which nursed by sows fed dietary ω6:ω3 ratio = 4:1 from G28 until the end of lactation. The ellipses represent 95% confidence region.

participated in RNA binding [GO:0003723], structural molecule activity [GO:0005198], and protein binding [GO:0005515]. The DAPs mostly located in extracellular space [GO:0005615], vesicle [GO:0031982], and cytosol [GO:0005829]. The top 20, 10, and 5 GO terms on BP, MF, and CC, respectively, are presented in Supplementary Fig. S4.

3.1.4. GO and Reactome pathway enrichment in LR vs CR groups

The DAP PPI network enrichment between LR and CR ileum was not significant ($p = 0.407$). So, the network was expanded with a maximum of 5 interactors in the first shell, and the result showed 10 nodes and 21 edges ($p = 0.0003$). GO analysis highlighted top three enriched BP terms were translational initiation [GO:0006413], cytoplasmic translation [GO:0002181], and transport [GO:0006810]. The top three enriched Reactome pathways were peptide chain elongation [HSA-156902], SRP-dependent co-translational protein targeting to membrane [HSA-1799339], and selenocysteine synthesis [HSA-2408557]. Lists of enriched GO terms and Reactome pathways are presented in Supplementary Table S2 and Supplementary Fig. S5.

3.1.5. GO and Reactome pathway enrichment in SW vs CT groups

The expanded PPI network with maximum 5 interactors in the first shell shows 24 nodes and 31 edges ($p = 0.0001$). The DAPs were particularly involved in cristae formation [GO:0042407], biosynthetic process [GO:0009058], and proton transmembrane transport [GO:1902600]. The top three enriched Reactome pathways were the formation of ATP by chemiosmotic coupling [HSA-163210], cristae formation [HSA-8949613], and the citric acid (TCA) cycle and respiratory electron transport [HSA-1428517]. Lists of enriched GO terms and Reactome pathways are presented in Supplementary Table S3 and Supplementary Fig. S6.

Additionally, a network among comparisons LR vs CR and SW vs CT provides an overview of the interaction between the DAPs and significantly enriched Reactome pathways (Fig. 5). This network presents the up- and down-regulated proteins distinctively for each comparison and their association with related Reactome pathways such as metabolism [HSA-1430728], developmental biology [HSA-1266738], and peptide chain elongation [HSA-156902].

3.1.6. GO and Reactome pathway enrichment in LRCT, CRSW, and LRSW vs CRCT groups

The PPI network enrichment in LRCT - CRCT comparison was not significant ($p = 0.221$). Thus, maximum 5 interactors were added in the first shell of the network to have 17 nodes and 22 edges ($p = 0.016$). The DAPs were involved in 13 BP, particularly response to stimulus [GO:0050896], regulation of cellular component organization [GO:0051128], and protein folding [GO:0006457]. The functional enrichment analysis highlighted 51 Reactome pathways, particularly the metabolism of proteins [HSA-392499], integration of energy metabolism [HSA-163685], and transport of small molecules [HSA-382551]. A list of enriched GO terms and Reactome pathways are shown in Supplementary Table S4 and Supplementary Fig. S7.

Comparing CRSW and CRCT ileum, the expanded PPI network with maximum 5 interactors in the first shell shows 31 nodes and 60 edges ($p = 2.84e-11$). In the expanded network, 15 GO-BP terms were highlighted, particularly transport [GO:0006810], biosynthetic process [GO:0009058], and export from cell [GO:0140352]. Twenty-three Reactome pathways were enriched, particularly the metabolism of proteins [HSA-392499], metabolism of amino acids and derivatives [HAS-71291], and cellular responses to stress [HAS-2262752]. A list of enriched GO terms and Reactome pathways are shown in Supplementary Table S5 and Supplementary Fig. S8.

The expanded PPI network in LRSW versus CRCT with maximum 5 interactors in the first shell shows 29 nodes and 51 edges ($p = 1.07e-07$). The top three enriched GO-BP terms were organonitrogen compound biosynthetic process [GO:1901566], transport [GO:0006810], and nuclear-transcribed mRNA catabolic process, nonsense-mediated decay [GO:0000184]. The top three enriched Reactome pathways were metabolism [HSA-1430728], formation of ATP by chemiosmotic coupling [HSA-163210], and peptide chain elongation [HSA-156902]. A list of enriched GO terms and Reactome pathways are shown in

Table 2
The differentially abundant proteins (DAPs) in piglet ileum at day 22 post-weaning among 4 groups containing CRCT, CRSW, LRCT and LRSW.

Protein name	Gene names	Accession number[1]	Number of peptides	log2FC[2]						*P*-value					
				CRSW vs CRCT	CRSW vs LRCT	LRCT vs CRCT	LRSW vs CRCT	LRSW vs CRSW	LRSW vs LRCT	CRSW vs CRCT	CRSW vs LRCT	LRCT vs CRCT	LRSW vs CRCT	LRSW vs CRSW	LRSW vs LRCT
Aconitate hydratase, mitochondrial (Aconitase)	ACO2	F1SRC5	2	−0.26	/	−0.17	−0.18	/	/	0.003	/	0.033	0.030	/	/
Neuroblast differentiation-associated protein AHNAK isoform X1**	AHNAK	A0A4X1VKL9	6	−0.16	/	/	/	/	/	0.021	/	/	/	/	/
4-rimethylaminobutyraldehyde dehydrogenase	ALDH9A1	F1S232	2	−0.33	/	/	−0.35	/	/	0.044	/	/	0.025	/	/
Fructose-bisphosphate aldolase	ALDOA	A0A4X1U0N5	11	0.08	/	/	0.10	/	/	0.039	/	/	0.016	/	/
AP-2 complex, beta subunit	AP2B1	A0A4X1T8Q4	2	/	/	0.34	/	/	/	/	/	0.017	/	/	/
Sodium/potassium-transporting ATPase subunit alpha	ATP1A1	A0A4X1SW39	2	−0.47	/	/	−0.59	/	/	0.038	/	/	0.012	/	/
ATP synthase subunit alpha	ATP5A1	A0A287AGU2	13	/	/	/	−0.15	/	−0.11	/	/	/	0.010	/	0.049
ATP synthase subunit beta	ATP5B	A0A481D142	17	/	/	/	−0.14	/	/	/	/	/	0.031	/	/
Calmodulin 1	CALM1	A0A4X1ST02	3	/	/	−0.12	−0.18	/	/	/	/	0.047	0.007	/	/
T-complex protein 1 subunit beta	CCT2	A0A5G2QMG1	2	/	/	/	0.24	0.20	/	/	/	/	0.011	0.025	/
T-complex protein 1 subunit theta	CCT8	A0A480X895	2	0.16	/	0.16	0.21	/	/	0.038	/	0.038	0.008	/	/
Collagen alpha-2(VI) chain isoform 2C2	COL6A2	A0A480W6C8	9	0.23	/	/	/	/	/	0.048	/	/	/	/	/
Coactosin-like protein 1	COTL1	A0A4X1T354	3	−0.31	−0.25	/	/	0.29	/	0.002	0.011	/	/	0.004	/
Cathepsin D	CTSD	A0A480M5F4	2	0.41	/	0.36	0.52	/	/	0.021	/	0.042	0.006	/	/
Decorin	DCN	F1SQ10	4	0.30	/	/	0.23	/	/	0.004	/	/	0.020	/	/
Dihydropyrimidinase-related protein 2	DPYSL2	G9F6X9	3	−0.16	/	−0.20	/	/	/	0.049	/	0.020	/	/	/
Enoyl coenzyme A hydratase 1	ECH1	A0A4X1T0M5	2	/	/	/	−0.81	/	−0.56	/	/	/	0.005	/	0.039
Fatty acid binding protein 6	FABP6	F1RR40	6	/	/	/	−0.55	/	/	/	/	/	0.017	/	/
Glutamine-fructose-6-phosphate transaminase	GFPT1	E1U318	2	/	/	/	/	0.54	/	/	/	/	/	0.015	/
G protein subunit beta 1	GNB1	A0A287A7Q3	2	/	/	−0.17	/	/	/	/	/	0.008	/	/	/
Histone H1.4	HIST1H1E	A0A480QWI4	8	/	/	/	0.44	/	/	/	/	/	0.023	/	/
Histone H2A	H2AX	A0A5G2QMX0	3	/	−0.67	/	/	/	/	/	0.017	/	/	/	/
Hemoglobin subunit beta	HBB	P02067	8	0.27	/	/	/	/	/	0.017	/	/	/	/	/
10 kDa heat shock protein, mitochondrial (Chaperonin 10)	HSPE1	F1SMZ6	4	0.21	/	/	/	/	/	0.044	/	/	/	/	/
Heparan sulfate proteoglycan 2	HSPG2	A0A287ATP0	4	/	/	/	/	/	0.24	/	/	/	/	/	0.035
Immunoglobulin lambda-like polypeptide 5 precursor*	IGLL5	A0A4X1T0Z9	2	/	/	/	/	0.93	/	/	/	/	/	0.048	/
Keratin, type I cytoskeletal 19	KRT19	A0A480IFL7	11	/	/	/	−0.72	−0.39	−0.62	/	/	/	0.001	0.040	0.003
Keratin, type I cytoskeletal 20	KRT20	A0A5G2QPZ4	6	/	/	/	−1.24	/	−0.90	/	/	/	0.001	/	0.012
Keratin, type II cytoskeletal 8	KRT8	A0A4X1WBI1	18	/	/	/	−0.82	/	−0.62	/	/	/	0.002	/	0.011
GST class-pi	LOC100739508	A0A287BQ81	4	/	/	/	−0.15	/	/	/	/	/	0.033	/	/
Moesin	MSN	A0A4X1VQZ3	5	/	/	/	/	/	0.10	/	/	/	/	/	0.032
Nucleoplasmin domain-containing protein	NPM1	A0A4X1U9Z4	6	/	/	/	0.24	/	/	/	/	/	0.018	/	/
Proliferating cell nuclear antigen	PCNA	X5FB24	2	/	0.54	/	/	/	0.56	/	0.047	/	/	/	0.029
PDZ and LIM domain protein 7	PDLIM7	A0A4X1SEG0	3	/	−0.24	/	/	/	/	/	0.017	/	/	/	/
6-phosphogluconate dehydrogenase, decarboxylating	PGD	A0A480YSA5	2	−0.32	/	/	/	/	/	0.046	/	/	/	/	/
Plectin (Fragment)	PLEC	K9IVQ6	3	/	/	/	/	0.15	/	/	/	/	/	0.047	/
Proteasome activator complex subunit 1	PSME1	Q64L94	4	−0.23	/	/	/	/	/	0.032	/	/	/	/	/
Ras-related protein Rab-10	RAB10	A0A4X1TSZ3	2	−0.16	/	/	/	/	/	0.033	/	/	/	/	/

(*continued on next page*)

Table 2 (*continued*)

Protein name	Gene names	Accession number[1]	Number of peptides	log2FC[2]						*P*-value					
				CRSW vs CRCT	CRSW vs LRCT	LRCT vs CRCT	LRSW vs CRCT	LRSW vs CRSW	LRSW vs LRCT	CRSW vs CRCT	CRSW vs LRCT	LRCT vs CRCT	LRSW vs CRCT	LRSW vs CRSW	LRSW vs LRCT
Ras-related protein Rap-1b	RAP1B	A0A5G2QA99	2	−0.12	/	/	/	/	/	0.045	/	/	/	/	/
60S ribosomal protein L10A	RPL10A	A0A4X1T0H0	2	0.22	/	/	/	/	/	0.039	/	/	/	/	/
Ribosomal protein L18 (Fragment)	RPL18	Q0QEV2	2	/	/	/	/	/	−0.34	/	/	/	/	/	0.033
TRASH domain-containing protein	RPL24	A0A287A286	2	0.35	/	/	/	/	/	0.042	/	/	/	/	/
40S ribosomal protein S3a	RPS3A	B6V8C8	3	/	/	/	0.22	/	/	/	/	/	0.036	/	/
40S ribosomal protein SA	RPSA	A0A480SME4	4	/	/	/	0.22	/	/	/	/	/	0.027	/	/
SERPINE1 mRNA binding protein 1	SERBP1	A0A5G2QNW1	2	/	/	/	/	/	0.60	/	/	/	/	/	0.045
Collagen-binding protein	SERPINH1	A0A480U2E1	10	0.12	0.09	/	0.08	/	/	0.004	0.016	/	0.033	/	/
Superoxide dismutase 1 (Fragment)	SOD1	Q95ME5	2	0.32	/	/	/	/	/	0.026	/	/	/	/	/
Stress-induced phosphoprotein 1	STIP1	A0A0B8RZ32	3	0.16	/	0.20	/	/	/	0.043	/	0.013	/	/	/
Vasodilator-stimulated phosphoprotein	VASP	A0A481C371	2	−0.20	/	−0.18	−0.15	/	/	0.012	/	0.021	0.047	/	/
Villin-1	VIL1	Q29261	2	/	/	/	−1.56	/	−1.18	/	/	/	0.007	/	0.014
14-3-3 protein theta	YWHAQ	A0A5G2QM17	7	/	/	−0.14	/	/	/	/	/	0.042	/	/	/

Protein names marked with * were shown as "Uncharacterized protein" in the UniProt *Sus scrofa* database, thus were substituted with the best match on *Sus scrofa* database, using SMARTBLAST tool.

[1] Accession number from UniProt protein database for *Sus scrofa*.

[2] log2FC is base 2 logarithm transformed of fold change value which represents the ratio of expression levels in the first-mentioned group vs second-mentioned group. CRCT: piglets fed no seaweed (SW, *Ascophyllum nodosum*), which nursed by sows fed dietary ω6:ω3 ratio = 13:1 during gestation, starting from day 28 (G28) and 10:1 during lactation. CRSW: piglets fed SW, which nursed by sows fed dietary ω6:ω3 ratio = 13:1 during gestation and 10:1 during lactation. LRCT: piglets fed no SW, which nursed by sows fed dietary ω6:ω3 ratio = 4:1 from G28 until the end of lactation. LRSW: piglets fed SW, which nursed by sows fed dietary ω6:ω3 ratio = 4:1 from G28 until the end of lactation.

Supplementary Table S6 and Supplementary Fig. S9.

3.2. Validation of proteomics results

Results of validation assays for villin (VIL1) and proliferating cell nuclear antigen (PCNA) are visualized in Fig. 6 and shown in Supplementary Table S7.

3.2.1. Villin (VIL1)

Western blot images for VIL1 in ileum samples from four groups of piglets are presented in Fig. 6 and Supplementary Table S7. Clear bands at 93 kDa showing the presence of VIL1 were detected in all samples. VIL1 band intensity in LR ileum was lower than in CR ileum (Fig. 6-A1, $p = 0.0497$), and VIL1 band intensity in SW ileum was lower than CT ileum (Fig. 6-A1, $p = 0.01$). A significantly lower concentration of VIL1 was determined in LRSW compared to CRCT ileum (Supplementary Table S7, $p = 0.016$). However, there was no interaction between the sow diet and the piglet diet. A strong positive linear correlation between validated VIL1 concentration and VIL1 relative abundance (Fig. 6-A2, $R = 0.87$, $p = 0.0027$) suggests an accurate reflection of VIL1 proteomics data level present in four piglet groups.

3.2.2. Proliferating cell nuclear antigen (PCNA)

Western blot analysis for PCNA is shown in Fig. 6 and Supplementary Table S7. Clear bands at 36 kDa representing the presence of PCNA were detected in all samples. PCNA band intensity in SW ileum was higher than CT ileum (Fig. 6-B1, $p = 0.01$), and this trend was shown in CRSW and CRCT groups (Supplementary Table S7, $p = 0.012$). There was a significant interaction between the sow diet and the piglet diet (Fig. 6-B1, $p = 0.03$): a significantly higher concentration of PCNA was determined in LRSW than the CRCT ileum (Supplementary Table S7, $p = 0.044$). The effect of the sow diet on the concentration of PCNA was not significant. The overall evaluation highlighted a strong positive linear correlation between the validated PCNA concentration and PCNA proteomics relative abundance (Fig. 6-B2, $R = 0.83$, $p = 0.0056$).

4. Discussion

Intestinal protective barrier and nutrient uptake are greatly affected by the continuous renewal of epithelial cells and crypt-villus structure [35]. Weaning induced significant alterations in intestinal structure and function [36] and hampered the immature mucosal immune system [3]. Factors such as maternal and offspring dietary management could drive mucosal immune development and progeny performance [37–39]. By investigating the combined effects of dietary treatments in sows and their offspring on offspring's development, this study aimed to stimulate a rapid maturation of the piglet intestine and immune system to resist weaning challenges. DAPs with modest differences (non-adjusted *p*-value < 0.05) were regarded as relevant because they are likely to give valid biological changes via validation assays on several proteins, as presented later. We hypothesized that the LR diet in the mothers would have an anti-inflammatory effect due to the higher ω3 and low ω6 content, and the SW diet in the piglets would inhibit oxidative damage by adding more bioactive compounds. It is noticed that we did not observe any evident signs of intestinal tissue damage between groups.

4.1. Effect of sow dietary treatments: LR vs CR groups

The maternal LR diet affected the relative abundance of GFPT1, CCT2, PDLIM7, RPSA, and CALM1. Proteins RPSA, CCT2, and GFPT1 were annotated by Reactome pathways referred to peptide chain elongation, selenocysteine synthesis, and metabolism of proteins.

Ribosomes contribute considerably to the host's response to infection [40] because this is where the message in mRNA is translated to proteins (also known as protein synthesis) [41]. The 40S ribosomal protein SA (RPSA) can contribute to the initiation step of mRNA

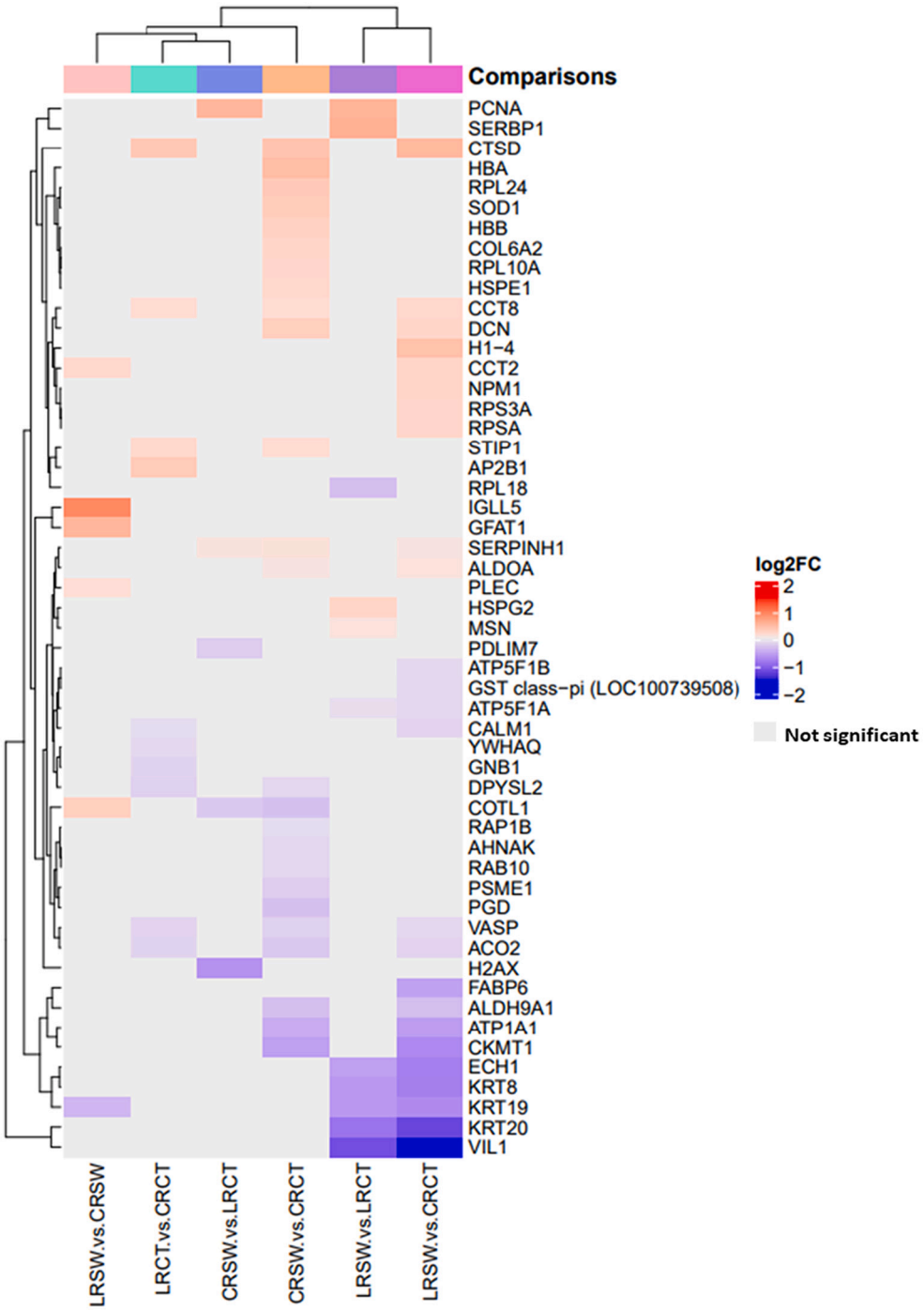

Fig. 4. Heatmap of the significant differentially abundant proteins (DAPs) among four groups of piglet ileum containing CRCT: piglets fed no seaweed (SW, *Ascophyllum nodosum*), which nursed by sows fed dietary ω6:ω3 ratio = 13:1 during gestation, starting from day 28 (G28) and 10:1 during lactation. CRSW: piglets fed SW, which nursed by sows fed dietary ω6:ω3 ratio = 13:1 during gestation and 10:1 during lactation. LRCT: piglets fed no SW, which nursed by sows fed dietary ω6:ω3 ratio = 4:1 from G28 until the end of lactation. LRSW: piglets fed SW, which nursed by sows fed dietary ω6:ω3 ratio = 4:1 from G28 until the end of lactation.

translation and trans-translation events [42]. The increased abundance of protein RPSA in LR versus CR ileum in this study may relate to the positive regulation of the protein synthesis process [41], thereby contributing to immune response activation [40]. Chaperonin-containing T-complex protein 1 (CCT) is a macromolecular protein folding complex that consists of eight subunit proteins (CCT1–8) [43] relating to cell cycling dysregulation and leading to uncontrolled proliferation [44]. The subunit beta (CCT2) may drive cell division and attract proliferative factors in humans, affecting crucial survival and growth components [44]. CCT2 can regulate cell proliferation; thus, the upregulation of CCT2 in LR versus CR ileum in this study can induce uncontrolled proliferation and is associated with the overexpression of cell cycle regulators [44]. Glutamine-fructose-6-phosphate transaminase (GFPT1) participates in protein glycosylation (glycans biosynthesis) which could enhance the solubility and stability of newly formed peptides [45]. The glycosylation process contributes to inflammation states, so GFPT1 protein plays a role in the host response to inflammation [46]. In this study, the changes in GFPT1 protein and, in turn, glycosylation process in LR versus CR ileum may relate to inflammatory conditions [46].

Taken together, the increased expression of RPSA, CCT2, and GFPT1 in LR ileum may relate to the host response to inflammatory stimuli and thus, affect piglet' growth performance, as observed in the in vivo study [14].

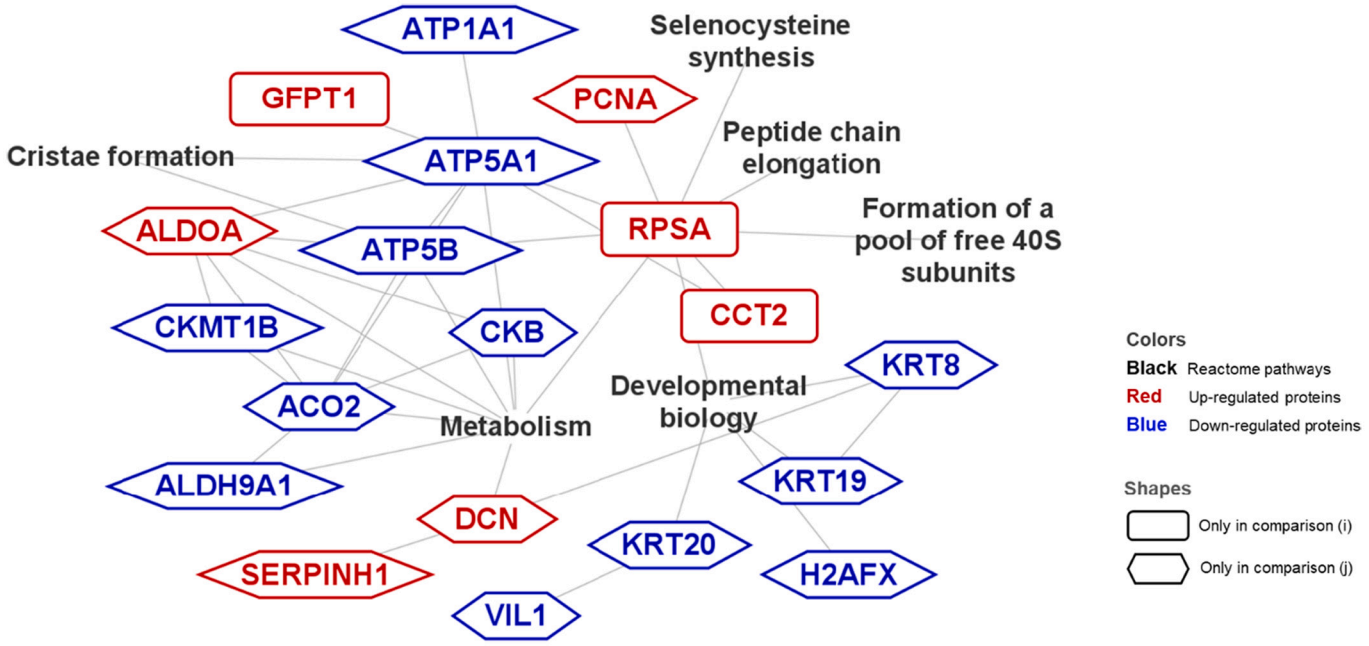

Fig. 5. Network of the significant differentially abundant proteins (DAPs) between two main comparisons of piglet ileum with significantly enriched Reactome pathways, containing comparisons LR vs CR and SW vs CT. Interaction networks were created with maximum 5 interactors shown in the first shell. CR: piglet born from sow fed diet with ω6:ω3 ratio = 13:1 during gestation, starting from day 28 (G28) and 10:1 during lactation; LR: piglet born from sow fed diet with ω6:ω3 ratio = 4:1 from G28 until the end of lactation. SW: piglet diet with seaweed supplementation, CT: piglet diet without seaweed supplementation.

4.2. Effect of piglet dietary treatments: SW vs CT groups

In the SW piglets, 11 proteins (i.e., ACO2, ATP5B, ATP5A1, DCN, CKB, CKMT1B, ALDH9A1, PSME1, ALDOA, PCNA) were annotated by Reactome pathways mostly referred to metabolism, the citric acid (TCA) cycle, and respiratory electron transport, synthesis of DNA, protein localization, mitochondrial protein import, and creatine metabolism.

Proliferating cell nuclear antigen (PCNA), a marker of cell proliferation [47], was upregulated in SW versus CT ileum (specifically, in CRSW and LRSW versus LRCT) in this study. The PCNA is an auxiliary protein of DNA polymerise-δ that participates in DNA synthesis, replication, and repair; cell proliferation, and cell cycle initiation [48,49]. The concentration of PCNA is decreased in the inactive cells; however, it increases before DNA replication [49]. PCNA is increased through phosphorylation during the cell cycle, so DNA replication and cellular proliferation are stimulated [47]. The increased expression of PCNA in the SW group could result from the increased proliferation behavior of cells [47], DNA synthesis, and repair associated with the SW diet.

Ileal epithelial keratin (KRT8, 19, and 20) and villin-1 (VIL1) were not involved in any Reactome pathways, but are the most significant down-regulated proteins, thus, relevant to mention the abundance pattern and possible biological meanings of these proteins as follows.

Keratin type II cytoskeletal 8 (KRT8, acidic keratin) and type I cytoskeletal 19 and 20 (KRT19 and 20, basic keratin) [50] were decreased expressions in SW piglets. Keratins are intermediate filament proteins expressed in epithelia of the gastrointestinal tract in mammals [51] that support the structure of cell and tissue homeostasis [52]. Keratins also contribute to the host protection against stress/inflammation [53,54] through maintaining epithelial barrier functions [55]. A review from Polari et al. [52] found that keratins alteration in expression level might contribute to the differentiation-proliferation balance of the epithelial cell. Protein K8 and K19 are the primary keratins in small and large intestines [52]. Furthermore, keratins are involved in many post-translational modifications (PTMs), so increased keratin expression was associated with cancer development where PTMs are dysregulated [54]. The decreased level of K8, K19, and K20 in SW ileum may relate to their role in epithelial cell metabolism [53] and the possible effect of SW on lowering the inflammation severity in post-weaning piglets.

Villin-1 (VIL1), an indicator of absorptive cells in the brush border [56], was decreased expressions in SW piglets (specifically, in LRSW versus CRCT and LRCT). The tendency of a down-regulation in villin mRNA expression was observed in the jejunal tissue of neonatal piglets on d7 versus d0, reflecting declined jejunal villus height of 7-d-old piglets [57]. This is one of the indicators of the fast intestinal development in suckling pigs, together with the increased villus width and number of crypts [57]. As located in the epithelial brush border, villin functions as a crucial regulator of epithelial structure and microvilli physiological functions [58]. Alteration of villin concentration may induce the remodelling of intestinal epithelial cells structure, and consequently, alter brush border integrity [58]. Microvilli development could enlarge the intestinal epithelial cells' contact area, absorption, and secretory surface [58].

The agreement between Western blot validation results and relative protein abundance measured by proteomics (Fig. 6, $R \geq 0.83$, $p < 0.01$) for both VIL1 and PCNA shows that despite the adjusted *p*-value giving no significant results, the non-adjusted *p*-values are likely giving valid biological changes. Validation on VIL1 and PCNA identified by two peptides and relatively low in abundance confirm crucial biologically relevant aspects disclosed by the TMT quantitative proteomics data [59]. This approach increases the confidence level in protein identification [59].

Collectively, the upregulation of PCNA and downregulation of VIL1 in SW piglets observed in this study suggests that SW supplementation stimulates the rapid renewal of the ileal epithelium by promoting cell proliferation but diminishes the absorption capacity of ileal epithelial cells at the same time.

4.3. Combined effects of sow and piglet dietary treatments: LRCT, CRSW, and LRSW vs CRCT groups

In the comparisons among 4 groups containing CRCT, CRSW, LRCT, and LRSW, a series of 6 pairwise comparisons revealed 53 DAPs, of which the majority of DAPs was in CRSW vs CRCT and LRSW vs CRCT (25 DAPs), followed by LRSW vs LRCT and LRCT vs CRCT (11 and 10

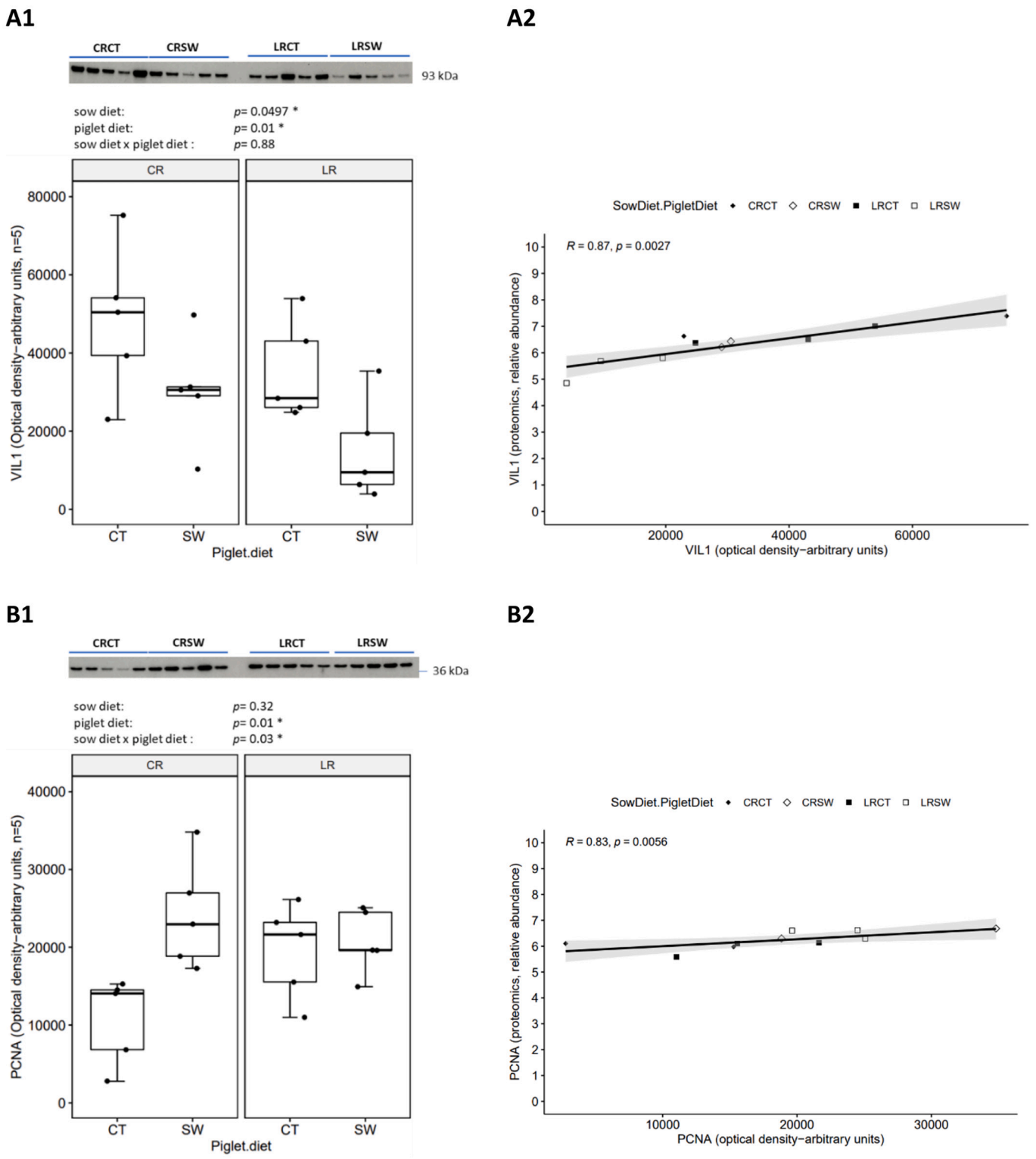

Fig. 6. Boxplots show results of validation assays for the concentrations of villin (VIL1) and proliferating cell nuclear antigen (PCNA) in ileum samples are presented with their correlation with respective protein abundance quantified by proteomics. CRCT: piglets fed no seaweed (SW, *Ascophyllum nodosum*), which nursed by sows fed dietary ω6:ω3 ratio = 13:1 during gestation, starting from day 28 (G28) and 10:1 during lactation. CRSW: piglets fed SW, which nursed by sows fed dietary ω6:ω3 ratio = 13:1 during gestation and 10:1 during lactation. LRCT: piglets fed no SW, which nursed by sows fed dietary ω6:ω3 ratio = 4:1 from G28 until the end of lactation. LRSW: piglets fed SW, which nursed by sows fed dietary ω6:ω3 ratio = 4:1 from G28 until the end of lactation.

DAPs, respectively), and the lowest DAPs was in LRSW vs CRSW and CRSW vs LRCT (6 and 5 DAPs, respectively). This discussion focuses on the distinct DAPs and associated Reactome pathways in two main comparisons: CRSW and LRSW vs CRCT groups with their expanded networks (maximum 5 interactors in the first shell).

The comparison between CRSW-CRCT allowed to identify 13 proteins such as COTL1, HBB, RAB10, RAP1B, RPL10A, RPL24, SOD1, PGD, and PSME1. These proteins were annotated by Reactome pathways

referred to the metabolism of proteins, RNA, and amino acids and derivatives, neutrophil degranulation, and cellular responses to stress. Ribosomal proteins such as RPL10A and RPL24 were overabundant in CRSW piglets, suggesting that supplementation with SW promotes protein synthesis and drives the regeneration of ileal tissue [60]. In addition, a negative regulator of the cell cycle/adhesion and mediator of protein degradation, proteasome activator complex subunit 1 (PSME1) [61,62], was downregulated in CRSW ileum. A protein that regulates actin cytoskeleton activity, coactosin-like protein 1 (COLT1) [63] can promote lamellipodia protrusion in motile cells such as endothelial, immune, and epithelial cells [64]. Both PSME1 and COTL1 were upregulated in inflammatory-, tumour- or cancer-associated events [62,65–69]. Referring to the benefits of CRSW diet on improving piglet growth performance as reported in the previous study [14], the downregulation of PSME1 and COTL1 in CRSW ileum had no harmful effects or their effects were masked from the positive effects of hemoglobin and ribosomal proteins.

In the LRSW vs CRCT piglets, 14 proteins (including ATP5A1, ATP5B, CCT2, ECH1, FABP6, KRT8, KRT19, KRT20, RPSA, and RPS3A) were annotated by Reactome pathways mostly referred to metabolism, organelle biogenesis and maintenance, developmental Biology, and protein localization. An enzyme that participates in mitochondrial fatty acid β-oxidation, Enoyl coenzyme A hydratase 1 (ECH1) [70] was downregulated in LRSW. This finding is supported by a previous study that reported the underlying beneficial effects of dietary ω3 PUFA supplementation in the insulin signalling improvement process via downregulating ECH1 and inhibiting peroxisomal β-oxidation [71]. LRSW piglets had downregulation of Fatty acid-binding protein 6 (FABP6) - an ileum-specific bile acid transporter, implicating a reduction in efficiency of dietary fat absorption [72,73] due to impaired bile acid production/absorption in ileum as a consequence of early inflammatory reaction [74,75]. A cell cycle-associated protein that organizes chromatin structure and regulates gene transcription via chromatin remodelling, Histone protein - HIST1H1E [76,77], although was not involved in any pathways, is still worth mentioning because its upregulation in LRSW piglets may facilitate DNA replication, DNA repair, and genome stability [77]. Together these observations suggest that the decreased fat absorption capacity may be associated with unexpected growth development of LRSW piglets as observed in the previous study [14], although they may have insulin signalling improvement and genome stability.

5. Conclusions

This study showed that maternal dietary low ω6:ω3 ratio (LR) exerted its positive regulation of protein synthesis process and contributed to enhanced intestinal function via modulating ileal proteome in piglets. However, maternal LR diet may induce uncontrolled proliferation and overexpression of cell cycle regulators in the offspring, which may be responsible for the lower growth performance of piglets, as shown in the in vivo experiment of this study. Seaweed (SW) supplementation can reduce inflammation severity and stimulate the rapid renewal of the ileal epithelium and ileal tissue development in CRSW piglets but diminish the fat absorption capacity of epithelial cells in LRSW piglets. Overall, lowering dietary ω6:ω3 ratio (to 4:1) in sows and SW supplementation in weaned piglet's diet benefitted piglet's intestinal development and anti-inflammation activity against weaning challenges. These results show that interaction between maternal and piglet diet could improve efficiency and drive pig production towards sustainable development by maintaining (improving) intestinal health.

Author contributions

Conceptualization: TXN, AA, GS, PDE, and RB; Funding acquisition and project administration: TXN, RB, DE, GS; Methodology and validation: TXN, SM, SW, QHH, AG, MM, RB, DE; Data curation: TXN, RB, DE; Formal analysis and interpretation of data: TXN; Writing - original draft: TXN; Writing - reviewing and editing: TXN, AA, QHH, AG, GS, DE, and RB; Approval of the final version to be submitted: TXN, AA, SM, SW, QHH, AG, MM, GS, DE, and RB.

Declaration of Competing Interest

The authors have no competing interests. The funder of the study had no role in study design, data collection, analyses, and interpretation; manuscript preparation, or decision to publish the results.

Data availability

Data will be made available on request.

Acknowledgments

This project is supported by the European Unions' Horizon 2020 research and innovation programme H2020-MSCA-ITN-2017-EJD under the Marie Skłodowska-Curie Innovative Training Networks (European Joint Doctorate in Molecular Animal Nutrition, MANNA), grant agreement No 765423.

Appendix A. Supplementary data

Supplementary data to this article can be found online at https://doi.org/10.1016/j.jprot.2022.104739.

References

[1] C. Xi, Y. Zehong, H. Huiling, D. Wentao, W. Aiping, D. Yanbin, G. Weihang, D. Song, C. Bo, L. Jiali, S. Nannan, C. Zhibin, G. Wenfeng, L. Yanwu, G. Yong, Differentiation and proliferation of intestinal stem cells and its underlying regulated mechanisms during weaning, Curr. Protein Pept. Sci. 20 (2019), https://doi.org/10.2174/1389203720666190125101834.

[2] N. Verdile, R. Mirmahmoudi, T.A.L. Brevini, F. Gandolfi, Evolution of pig intestinal stem cells from birth to weaning, Animal. 13 (2019) 2830–2839, https://doi.org/10.1017/S1751731119001319.

[3] C.R. Stokes, The development and role of microbial-host interactions in gut mucosal immune development, J. Anim. Sci. Biotechnol. 8 (2017) 8–17, https://doi.org/10.1186/s40104-016-0138-0.

[4] F. Correa, D. Luise, P. Bosi, P. Trevisi, Weaning differentially affects the maturation of piglet peripheral blood and jejunal Peyer's patches, Sci. Rep. 12 (2022) 1–12, https://doi.org/10.1038/s41598-022-05707-9.

[5] T.A. Mousseau, C.W. Fox, The adaptive significance of maternal effects, Trends Ecol. Evol. 13 (1998) 403–407, https://doi.org/10.1016/S0169-5347(98)01472-4.

[6] L.M. Dixon, N.H.C. Sparks, K.M.D. Rutherford, Early experiences matter: A review of the effects of prenatal environment on offspring characteristics in poultry, Poult. Sci. 95 (2016) 489–499, https://doi.org/10.3382/ps/pev343.

[7] E.H. Van Der Waaij, H. Van Den Brand, J.A.M. Van Arendonk, B. Kemp, Effect of match or mismatch of maternal-offspring nutritional environment on the development of offspring in broiler chickens, Animal. 5 (2011) 741–748, https://doi.org/10.1017/S1751731110002387.

[8] J. Fisch, V. Feistauer, A.C. de Moura, A.O. Silva, V. Bollis, M. Porawski, S. Almeida, R.P. Guedes, A.G. Barschak, M. Giovenardi, Maternal feeding associated to post-weaning diet affects metabolic and behavioral parameters in female offspring, Physiol. Behav. 204 (2019) 162–167, https://doi.org/10.1016/j.physbeh.2019.02.026.

[9] C.W. Kuzawa, A.W. Kim, Early Environments, Developmental Plasticity, and Chronic Degenerative Disease, Elsevier Inc., 2022, https://doi.org/10.1016/b978-0-12-822652-0.00020-1.

[10] J.J. DiNicolantonio, J. O'Keefe, The importance of maintaining a low Omega-6/Omega-3 ratio for reducing the risk of inflammatory cytokine storms, Mo. Med. 117 (2020) 539–542.

[11] A.P. Simopoulos, An increase in the Omega-6/Omega-3 fatty acid ratio increases the risk for obesity, Nutrients. 8 (2016) 1–17, https://doi.org/10.3390/nu8030128.

[12] J.J. Dinicolantonio, J. O'keefe, J.H. O'keefe, The Importance of Maintaining a Low Omega-6/Omega-3 Ratio for Reducing the Risk of Autoimmune Diseases, Asthma, and Allergies, Mo. Med. 118 (2021) 453. /pmc/articles/PMC8504498/%0A/pmc/articles/PMC8504498/?report=abstract%0Ahttps://www.ncbi.nlm.nih.gov/pmc/articles/PMC8504498/.

[13] R.K. Saini, Y.S. Keum, Omega-3 and omega-6 polyunsaturated fatty acids: Dietary sources, metabolism, and significance — A review, Life Sci. 203 (2018) 255–267, https://doi.org/10.1016/j.lfs.2018.04.049.

[14] T.X. Nguyen, A. Agazzi, M. Comi, V. Bontempo, I. Guido, S. Panseri, H. Sauerwein, P.D. Eckersall, R. Burchmore, G. Savoini, Effects of Low ω 6 : ω 3 Ratio in Sow Diet and Seaweed Supplement in Piglet Diet on Performance, Colostrum and Milk Fatty

Acid Profiles, and Oxidative Status, Animals. 10 (2020), https://doi.org/10.3390/ani10112049.
[15] A. Heras-molina, J.L. Pesántez-pacheco, C. Garcia-contreras, M. Vázquez-gómez, A. López, R. Benítez, Y. Núñez, S. Astiz, C. Óvilo, B. Isabel, A. González-bulnes, Maternal supplementation with polyphenols and omega-3 fatty acids during pregnancy: Prenatal effects on growth and metabolism, Animals. 11 (2021), https://doi.org/10.3390/ani11061699.
[16] H.Y. Sun, I.H. Kim, Coated omega-3 fatty acid from linseed oil positively affect sow immunoglobulin G concentration and pre-weaning performance of piglet, Anim. Feed Sci. Technol. 269 (2020), 114676, https://doi.org/10.1016/j.anifeedsci.2020.114676.
[17] L.M.S. Bouwman, J.M.S. Fernandez-Calleja, H.J.M. Swarts, I. van der Stelt, A. Oosting, J. Keijer, E.M. van Schothorst, No adverse programming by post-weaning dietary fructose of body weight, adiposity, glucose tolerance, or metabolic flexibility, Mol. Nutr. Food Res. 62 (2018) 1–10.
[18] B. Venardou, J.V. O'doherty, M. Garcia-Vaquero, C. Kiely, G. Rajauria, M. J. McDonnell, M.T. Ryan, T. Sweeney, Evaluation of the antibacterial and prebiotic potential of Ascophyllum nodosum and its extracts using selected bacterial members of the pig gastrointestinal microbiota, Mar. Drugs. 20 (2022), https://doi.org/10.3390/md20010041.
[19] J. Michiels, E. Skrivanova, J. Missotten, A. Ovyn, J. Mrazek, S. De Smet, N. Dierick, Intact brown seaweed (Ascophyllum nodosum) in diets of weaned piglets : effects on performance, gut bacteria and morphology and plasma oxidative status, J. Anim. Physiol. Anim. Nutr. (Berl). 96 (2012) 1101–1111, https://doi.org/10.1111/j.1439-0396.2011.01227.x.
[20] J.L. Turner, S.S. Dritz, J.J. Higgins, J.E. Minton, Effects of Ascophyllum nodosum extract on growth performance and immune function of young pigs challenged with Salmonella typhimurium, J. Anim. Sci. 80 (2002) 1947–1953, https://doi.org/10.2527/2002.8071947x.
[21] N. Dierick, A. Ovyn, S. De Smet, Effect of feeding intact brown seaweed Ascophyllum nodosum on some digestive parameters and on iodine content in edible tissues in pigs, J. Sci. Food Agric. 89 (2009) 584–594, https://doi.org/10.1002/jsfa.3480.
[22] D.M. Ribeiro, C.F. Martins, J. Kuleš, A. Horvatić, N. Guillemin, J.P.B. Freire, P. D. Eckersall, A.M. Almeida, J.A.M. Prates, Influence of dietary Spirulina inclusion and lysozyme supplementation on the longissimus lumborum muscle proteome of newly weaned piglets, J. Proteomics. 244 (2021), 104274, https://doi.org/10.1016/j.jprot.2021.104274.
[23] K. Yu, M. Matzapetakis, A. Horvatić, M. Terré, A. Bach, J. Kuleš, N. Yeste, N. Gómez, L. Arroyo, E. Rodríguez-tomàs, R. Peña, N. Guillemin, A.M. De Almeida, P. David, A. Bassols, Metabolome and proteome changes in skeletal muscle and blood of pre- weaning calves fed leucine and threonine supplemented diets, J. Proteomics. 216 (2020), 103677, https://doi.org/10.1016/j.jprot.2020.103677.
[24] S. Martinez-Subiela, A. Horvatic, D. Escribano, L. Pardo-Marin, M. Kocaturk, V. Mrljak, R. Burchmore, J.J. Ceron, Z. Yilmaz, Identification of novel biomarkers for treatment monitoring in canine leishmaniosis by high-resolution quantitative proteomic analysis, Vet. Immunol. Immunopathol. 191 (2017) 60–67, https://doi.org/10.1016/j.vetimm.2017.08.004.
[25] Y. Perez-Riverol, A. Csordas, J. Bai, M. Bernal-Llinares, S. Hewapathirana, D. J. Kundu, A. Inuganti, J. Griss, G. Mayer, M. Eisenacher, E. Pérez, J. Uszkoreit, J. Pfeuffer, T. Sachsenberg, Ş. Yilmaz, S. Tiwary, J. Cox, E. Audain, M. Walzer, A. F. Jarnuczak, T. Ternent, A. Brazma, J.A. Vizcaíno, The PRIDE database and related tools and resources in 2019: Improving support for quantification data, Nucleic Acids Res. 47 (2019) D442–D450, https://doi.org/10.1093/nar/gky1106.
[26] R. Baka, D. Eckersall, A. Horvatic, A. Gelemanovic, V. Mrljak, M. McLaughlin, L. V. Athanasiou, N. Papaioannou, I. Stylianaki, H.Q. Hanh, C.C. Chadwick, Z. Polizopoulou, Quantitative proteomics of cerebrospinal fluid using tandem mass tags in dogs with recurrent epileptic seizures, J. Proteomics. 231 (2021), 103997, https://doi.org/10.1016/j.jprot.2020.103997.
[27] T. Huang, M. Choi, M. Tzouros, S. Golling, N.J. Pandya, B. Banfai, T. Dunkley, O. Vitek, T. Huang, M. Choi, M. Tzouros, S. Golling, MSstatsTMT: statistical detection of differentially abundant proteins in experiments with isobaric labeling and multiple mixtures, Mol. Cell. Proteomics 19 (2020) 1706–1723, https://doi.org/10.1074/mcp.RA120.002105.
[28] T. R Core Team, R: A Language and Environment for Statistical Computing - Reference Index - Version 4.1.0 (2021-05-18), 2021, pp. 1–3728.
[29] H. Wickham, ggplot2: Elegant Graphics for Data Analysis, Second edition, Springer, 2016. http://link.springer.com/10.1007/978-0-387-98141-3.
[30] K.-A. Le Cao, F. Rohart, S.D. Ignacio Gonzalez, A.J. Abadi, B. Gautier, F. Bartolo, P. Monget, J. Coquery, F. Yao, B. Liquet, Package 'mixOmics, 2021.
[31] J.C. Oliveros, Venny. An Interactive Tool for Comparing Lists with Venn's Diagrams. https://bioinfogp.cnb.csic.es/tools/venny/index.html, 2021.
[32] D. Szklarczyk, A.L. Gable, K.C. Nastou, D. Lyon, R. Kirsch, S. Pyysalo, N. T. Doncheva, M. Legeay, T. Fang, P. Bork, L.J. Jensen, C. Von Mering, The STRING database in 2021 : Customizable protein – protein networks, and functional characterization of user-uploaded gene / measurement sets, Nucleic Acids Res. 49 (2021) 605–612, https://doi.org/10.1093/nar/gkaa1074.
[33] F. Supek, M. Bošnjak, N. Skunca, T. Šmuc, REVIGO summarizes and visualizes long lists of Gene Ontology terms, PLoS One 6 (2011), e21800, https://doi.org/10.1371/journal.pone.0021800.
[34] P. Shannon, A. Markiel, O. Ozier, N.S. Baliga, J.T. Wang, D. Ramage, N. Amin, B. Schwikowski, T. Ideker, Cytoscape: a software environment for integrated models of biomolecular interaction networks, Genome Res. 13 (2003) 2498–2504, https://doi.org/10.1101/gr.1239303.metabolite.
[35] H. Gehart, H. Clevers, Tales from the crypt: new insights into intestinal stem cells, Nat. Rev. Gastroenterol. Hepatol. 16 (2018) 19–34, https://doi.org/10.1038/s41575-018-0081-y.
[36] M. Wang, L. Wang, X. Tan, L. Wang, X. Xiong, Y. Wang, Q. Wang, H. Yang, Y. Yin, The developmental changes in intestinal epithelial cell proliferation, differentiation, and shedding in weaning piglets, Anim. Nutr. (2022), https://doi.org/10.1016/j.aninu.2021.11.006.
[37] C.N. Hsu, Y.L. Tain, Early-life programming and reprogramming of adult kidney disease and hypertension: The interplay between maternal nutrition and oxidative stress, Int. J. Mol. Sci. 21 (2020), https://doi.org/10.3390/ijms21103572.
[38] Q. Shang, S. Liu, H. Liu, S. Mahfuz, X. Piao, Maternal supplementation with a combination of wheat bran and sugar beet pulp during late gestation and lactation improves growth and intestinal functions in piglets, Food Funct. 12 (2021) 7329–7342, https://doi.org/10.1039/d1fo00014d.
[39] S. Wang, C.A. Maxwell, N.M. Akella, Diet as a potential moderator for genome stability and immune response in pediatric leukemia, Cancers (Basel). 13 (2021) 1–17, https://doi.org/10.3390/cancers13030413.
[40] J. Wei, A. Hui, Review of ribosome interactions with SARS-CoV-2 and COVID-19 mRNA vaccine, Life. 12 (2022), https://doi.org/10.3390/life12010057.
[41] R.A. Hall, E.W.J. Wallace, Post-transcriptional control of fungal cell wall synthesis, Cell Surf. 8 (2022), 100074, https://doi.org/10.1016/j.tcsw.2022.100074.
[42] A. Wadood, A. Shareef, A.U. Rehman, S. Muhammad, B. Khurshid, R.S. Khan, S. Shams, S.G. Afridi, In silico drug designing for ala438 deleted ribosomal protein S1 (RpsA) on the basis of the active compound Zrl 15, ACS Omega. 7 (2022) 397–408, https://doi.org/10.1021/acsomega.1c04764.
[43] Q. Liu, Y. Qi, X. Kong, X. Wang, W. Zhang, J. Zhai, Y. Yang, Y. Fang, J. Wang, Molecular and clinical characterization of CCT2 expression and prognosis via large-scale transcriptome profile of breast cancer, Front. Oncol. 11 (2021), https://doi.org/10.3389/fonc.2021.614497.
[44] H. Ghozlan, A. Showalter, E. Lee, X. Zhu, A.R. Khaled, Chaperonin-containing TCP1 complex (CCT) promotes breast cancer growth through correlations with key cell cycle regulators, front, Oncol. 11 (2021) 1–24, https://doi.org/10.3389/fonc.2021.663877.
[45] A.G. Engel, Congenital myasthenic syndromes in 2018, Curr. Neurol. Neurosci. Rep. 18 (2018), https://doi.org/10.1007/s11910-018-0852-4.
[46] I. Tvaroška, Glycosyltransferases as targets for therapeutic intervention in cancer and inflammation: molecular modeling insights, Versita (2022), https://doi.org/10.1007/s11696-021-02026-7.
[47] E. Chen, N.J. Liu, Y. Zhao, M. Tang, L.P. Ou, X.H. Wu, C.L. Luo, Panobinostat reverses HepaCAM gene expression and suppresses proliferation by increasing histone acetylation in prostate cancer, Gene. 808 (2022), 145977, https://doi.org/10.1016/j.gene.2021.145977.
[48] H.D. Nguyen, A.-K. Bielinsky, HDM2 ERKs PCNA, J. Cell Biol. 190 (2010) 487–489, https://doi.org/10.1002/jcc.20084.
[49] H. Tamura, Expression of p63 and proliferating cell nuclear antigen in oral submucous fibrosis, J. Int. Soc. Prev. Community Dent. 11 (2021) 448–456, https://doi.org/10.4103/jispcd.JISPCD.
[50] S. Werner, L. Keller, K. Pantel, Molecular aspects of medicine epithelial keratins: Biology and implications as diagnostic markers for liquid biopsies, Mol. Asp. Med. 72 (2020), 100817, https://doi.org/10.1016/j.mam.2019.09.001.
[51] C.-G. Stenvall, A. Tayyab, T. Mina, M.A. Grönroos, K. Ilomäki, K.M. Viiri, L. Ridge, D.M. Toivola Polari, Targeted deletion of keratin 8 in intestinal epithelial cells disrupts tissue integrity and predisposes to tumorigenesis in the colon, Cell. Mol. Life Sci. 79 (2022) 1–17, https://doi.org/10.1007/s00018-021-04081-5.
[52] L. Polari, C.M. Alam, J.H. Nyström, T. Heikkilä, M. Tayyab, S. Baghestani, D. M. Toivola, Keratin intermediate filaments in the colon: guardians of epithelial homeostasis, Int. J. Biochem. Cell Biol. 129 (2020), https://doi.org/10.1016/j.biocel.2020.105878.
[53] T.O. Helenius, J.O. Misiorek, J.H. Nyström, L.E. Fortelius, A. Habtezion, J. Liao, M. N. Asghar, H. Zhang, S. Azhar, M.B. Omary, D.M. Toivola, Keratin 8 absence down-regulates colonocyte HMGCS2 and modulates colonic ketogenesis and energy metabolism, Mol. Biol. Cell 26 (2015) 2298–2310, https://doi.org/10.1091/mbc.E14-02-0736.
[54] C.A. Evans, B.M. Corfe, Seminars in cell and developmental biology colorectal keratins : Integrating nutrition, metabolism and colorectal health, Semin. Cell Dev. Biol. (2021), https://doi.org/10.1016/j.semcdb.2021.08.010.
[55] L. Wang, S. Srinivasan, A.L. Theiss, D. Merlin, S.V. Sitaraman, Interleukin-6 induces keratin expression in intestinal epithelial cells: Potential role of keratin-8 in interleukin-6-induced barrier function alterations, J. Biol. Chem. 282 (2007) 8219–8227, https://doi.org/10.1074/jbc.M604068200.
[56] C. Zhong, D. Tong, Y. Zhang, X. Wang, H. Yan, H. Tan, C. Gao, DL -methionine and DL -methionyl- DL -methionine increase intestinal development and activate Wnt / b -catenin signaling activity in domestic pigeons (Columba livia), Poult. Sci. 101 (2019), 101644, https://doi.org/10.1016/j.psj.2021.101644.
[57] L. Yin, J. Li, Y. Zhang, Q. Yang, C. Yang, Z. Yi, Y. Yin, Q. Wang, J. Li, N. Ding, Z. Zhang, H. Yang, Y. Yin, Changes in progenitors and differentiated epithelial cells of neonatal piglets, Anim. Nutr. 8 (2022) 265–276, https://doi.org/10.1016/j.aninu.2021.10.008.
[58] D. Delacour, J. Salomon, S. Robine, D. Louvard, Plasticity of the brush border — the yin and yang of intestinal homeostasis, Nat. Rev. Gastroenterol. Hepatol. (2016), https://doi.org/10.1038/nrgastro.2016.5.
[59] D.C. Handler, D. Pascovici, M. Mirzaei, V. Gupta, G.H. Salekdeh, P.A. Haynes, The art of validating quantitative proteomics data, Proteomics. 18 (2018), https://doi.org/10.1002/pmic.201800222.
[60] Y. Jia, L. Li, Y. Lin, D.J. Siegwart, J.M. Ready, Y. Jia, L. Li, Y. Lin, P. Gopal, S. Shen, K. Zhou, X. Yu, T. Sharma, In vivo CRISPR screening identifies BAZ2 chromatin

remodelers as druggable regulators of mammalian liver regeneration, Cell Stem Cell 29 (2022) 1–14, https://doi.org/10.1016/j.stem.2022.01.001.
[61] Z. Mbita, R. Hull, F. Mokoena, C. Lai, Z. Dlamini, RBBP6 interactome: RBBP6 isoform 3/DWNN and Nek6 interaction is critical for cell cycle regulation and may play a role in carcinogenesis, Informat. Med. Unlocked. 23 (2021), 100522, https://doi.org/10.1016/j.imu.2021.100522.
[62] Q. Wang, F. Pan, S. Li, R. Huang, X. Wang, S. Wang, X. Liao, The prognostic value of the proteasome activator subunit gene family in skin cutaneous melanoma, J. Cancer 10 (2019) 2205–2219, https://doi.org/10.7150/jca.30612.
[63] F.A. Simmen, Y. Su, R. Xiao, Z. Zeng, The Krüppel-like factor 9 (KLF9) network in HEC-1-A endometrial carcinoma cells suggests the carcinogenic potential of dysregulated KLF9 expression, Reprod. Biol. Endocrinol. 6 (2008) 1–11, https://doi.org/10.1186/1477-7827-6-41.
[64] J. Kim, M.J. Shapiro, A.O. Bamidele, P. Gurel, P. Thapa, H.N. Higgs, K.E. Hedin, V. S. Shapiro, D.D. Billadeau, Coactosin-like 1 antagonizes Cofilin to promote lamellipodial protrusion at the immune synapse, PLoS One 9 (2014) 1–11, https://doi.org/10.1371/journal.pone.0085090.
[65] S. Guo, P. Yang, X. Jiang, X. Li, Y. Wang, Genetic and epigenetic silencing of mircoRNA-506-3p enhances COTL1 oncogene expression to foster non-small lung cancer progression, Oncotarget. 8 (2017) 644–657.
[66] E. Jin, S. Shim, H. Kim, S. Chae, Polymorphisms of COTL1 gene identified by proteomic approach and their association with autoimmune disorders, Exp. Mol. Med. 41 (2009) 354–361, https://doi.org/10.3858/emm.2009.41.5.040.
[67] S. Rai, S. Bhatnagar, Hyperlipidemia, disease associations, and top 10 potential drug targets: A network view, Omi. A J. Integr. Biol. 20 (2016) 152–169, https://doi.org/10.1089/omi.2015.0172.
[68] Y. Guo, X. Dong, J. Jin, Y. He, The expression patterns and prognostic value of the proteasome activator subunit gene family in gastric cancer based on integrated analysis, Front. Cell Dev. Biol. 9 (2021), https://doi.org/10.3389/fcell.2021.663001.
[69] S. Ge, H. Huang, W. Huang, R. Ji, J. Chen, S. Wu, L. Wang, PSME4 activates mTOR signaling and promotes the malignant progression of hepatocellular carcinoma, Int. J. Gen. Med. 15 (2022) 885–895.
[70] A. Braeuning, A. Oberemm, J. Görte, L. Böhmert, S. Juling, Comparative proteomic analysis of silver nanoparticle effects in human liver and intestinal cells, J. Appl. Toxicol. 38 (2018) 638–648, https://doi.org/10.1002/jat.3568.
[71] A. Camargo, O.A. Rangel-zúñiga, P. Peña-orihuela, C. Marín, P. Pérez-martínez, J. Delgado-lista, F.M. Gutierrez-mariscal, M.M. Malagón, H.M. Roche, F. José, F. Perez-jimenez, J. Lopez-miranda, Postprandial changes in the proteome are modulated by dietary fat in patients with, J. Nutr. Biochem. 24 (2013) 318–324, https://doi.org/10.1016/j.jnutbio.2012.06.014.
[72] S.M. Habib, B.L. Zwicker, L. Wykes, L.B. Agellon, Sexually dimorphic response of mice to the Western-style diet caused by deficiency of fatty acid binding protein 6 (Fabp6), Phys. Rep. 9 (2021) 1–10, https://doi.org/10.14814/phy2.14733.
[73] S. Peng, Y. Li, Q. Chen, Q. Hu, Y. He, L. Che, P. Jiang, Intestinal and mucosal microbiome response to oral challenge of enterotoxigenic Escherichia coli in weaned pigs, Pathogens. 11 (2022) 1–12.
[74] J.H. Uribe, M.C. Romero, S.Z. López, C. Arce, R. Bautista, A. Carvajal, S. Cirera, M. G. Claros, J.J. Garrido, Transcriptional analysis of porcine intestinal mucosa infected with Salmonella typhimurium revealed a massive inflammatory response and disruption of bile acid absorption in ileum, Vet. Res. 47 (2016) 1–10, https://doi.org/10.1186/s13567-015-0286-9.
[75] S. Gilani, G.S. Howarth, G. Nattrass, S.M. Kitessa, R. Barekatain, R.E.A. Forder, C. D. Tran, R.J. Hughes, Gene expression and morphological changes in the intestinal mucosa associated with increased permeability induced by short-term fasting in chickens, J. Anim. Physiol. Anim. Nutr. (Berl). 102 (2018) 653–661, https://doi.org/10.1111/jpn.12808.
[76] S.H. Yoon, J. Choi, W.J. Lee, J.T. Do, Genetic and epigenetic etiology underlying autism spectrum disorder, J. Clin. Med. 9 (2020) 1–27.
[77] C. Cytrynbaum, S. Choufani, R. Weksberg, Epigenetic signatures in overgrowth syndromes: Translational opportunities, Anim. J. Med. Genet. 181C (2019) 491–501, https://doi.org/10.1002/ajmg.c.31745.